Journal of The Electrochemical Society, **158** (4) D196-D199 (2011)
0013-4651/2011/158(4)/D196/4/$28.00 © The Electrochemical Society

Etched Surface Morphology of Heteroepitaxial Nonpolar $(11\bar{2}0)$ and Semipolar $(11\bar{2}2)$ GaN Films by Photoenhanced Chemical Wet Etching

Kwang Hyeon Baik,[a,z] Hoo-Young Song,[a] Sung-Min Hwang,[a] Younghun Jung,[b] Jaehui Ahn,[b] and Jihyun Kim[b,*,z]

[a]*Optoelectronics Laboratory, Korea Electronics Technology Institute, Seongnam, Gyeonggi 463-816, Korea*
[b]*Department of Chemical and Biological Engineering, Korea University, Seoul 136-701, Korea*

We investigated how selective wet etching changes the surface morphologies of nonpolar a-plane $(11\bar{2}0)$ and semipolar $(11\bar{2}2)$ GaN films grown on sapphire substrates. Trigonal prisms with various widths are seen on the top surface and the tapered sidewall facet of the a-plane GaN films along the c-axis direction. Inclined trigonal unit cells are observed on the semipolar $(11\bar{2}2)$ GaN films after wet etching. The specific crystallographic planes of $(10\bar{1}0)$, $(01\bar{1}0)$, and (0001) were exposed in common for both the GaN films, indicating that these planes are chemically stable due to atomic bond configurations and smaller density of atoms. Photoenhanced chemical wet etching proceeds on the a-plane and semipolar GaN films until chemically stable m-plane GaN surfaces as well as c-plane GaN surfaces are exposed.
 [DOI: 10.1149/1.3544916]

Manuscript submitted October 28, 2010; revised manuscript received December 29, 2010. Published February 22, 2011.

Nitride-based light-emitting diodes (LEDs) on nonpolar crystal orientations have received increasing attentions over the past several years due to their promise of removing the quantum-confined Stark effect. This polarization-related electric field induces electron and hole wavefunctions to be spatially separated in strained quantum well (QW) structure, leading to a reduced optical transition probability.[1–3] The absence of an internal electric field in a nonpolar gallium nitride (GaN) LEDs is advantageous to achieve not only highly efficient light emitters with thicker QWs but also improved wavelength stability with injection currents. Many research groups have successfully demonstrated nonpolar a-plane $(11\bar{2}0)$ and m-plane $(1\bar{1}00)$ GaN LEDs as well as semipolar $(10\bar{1}1)$ and $(11\bar{2}2)$ GaN LEDs.[4–11] Masui et al. had recently reported a comprehensive review on achievements and challenges on nonpolar and semipolar nitride LEDs.[12]

Photoenhanced chemical (PEC) wet etching on GaN is now commonly used in vertical thin-film GaN LEDs due to its simple and damage-free etching process.[13,15,16] The surface texturing with numerous hexagonal pyramids on nitrogen-face GaN films is one of the most effective ways to increase the extraction efficiency in high power GaN LEDs among various extraction methods, including highly reflective p-electrode, chip geometry deformation, patterned sapphire substrate, photonic crystals, and p-GaN surface roughening. There were previous papers that PEC wet etching could be also implemented in nonpolar and semipolar GaN films by selectively etching different crystallographic planes.[17–20] Hardy et al. recently demonstrated nonpolar m-plane superluminescent diodes by forming hexagonal pyramids on –c-face $(000\bar{1})$ via PEC etching.[19] However, there are few papers available on PEC wet etching on the nonpolar and semipolar GaN films. In this work, we studied how selective wet etching changes the surface morphologies of the nonpolar a-plane $(11\bar{2}0)$ and semipolar $(11\bar{2}2)$ GaN films grown on sapphire substrates.

Experimental

Nonpolar a-plane $(11\bar{2}0)$ GaN (a-GaN) and semipolar $(11\bar{2}2)$ GaN (s-GaN) films were grown on r-plane $(1\bar{1}02)$ and m-plane sapphire substrates by metallorganic chemical vapor deposition, respectively. In order to produce high crystalline quality films, the multi-buffer growth technique was employed with a high-temperature GaN nucleation layer. Prior to the growth, the substrate was thermally cleaned at 1050°C for 10 min, and the surface nitridation was carried out with an ammonia flow of 8 slm (stand liter per minute). A 150-nm thick GaN nucleation layer was grown in mixed atmosphere of N_2 and H_2 at an elevated temperature of 1050°C to obtain a minimum surface roughness and to reduce dislocation density. Subsequently, a 4.5-mm thick a-plane GaN template with a high crystalline quality surface was obtained by the conventional two-step growth method. During the three-dimensional (3D) island growth, a thin SiN_x layer was inserted by flowing SiH_4 and NH_3 to increase the crystal quality. The detailed growth conditions had been previously reported.[4] Both the nonpolar a-GaN and semipolar s-GaN films were immersed in a potassium hydroxide (KOH) solution at 4 M KOH concentrations for different periods of time. PEC etchings were performed at a stirring rate of 300 rpm at 60°C with ultraviolet illuminations. The etched surface morphologies of the a-GaN and s-GaN films were analyzed by a field emission scanning electron microscope (SEM).

Results and Discussion

Figure 1 shows a bird's-eye view SEM image of etched surface morphology having numerous hexagonal pyramids with facets of $\{10\bar{1}\bar{1}\}$ planes on the nitrogen-face GaN $(000\bar{1})$ films. It is well established that this surface texturing dramatically improves the light extractions in vertical thin-film GaN LEDs.[21,22] Li et al. reported that the wet etching of N-face GaN surface was related with the repetitive process of the oxidation and the dissolution of the gallium oxide via hydroxide ions (OH^-) in alkali solutions.[23] They also suggested that

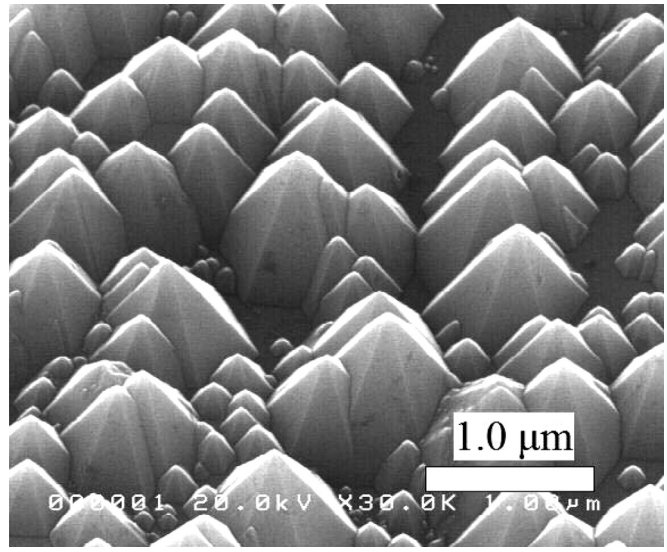

Figure 1. A tilted SEM image of c-plane N-face GaN after PEC wet etching. Numerous hexagonal pyramids with $\{10\bar{1}\bar{1}\}$ facets are observed.

* Electrochemical Society Active Member.
z E-mail: khbaik@keti.re.kr; hyunhyun7@korea.ac.kr

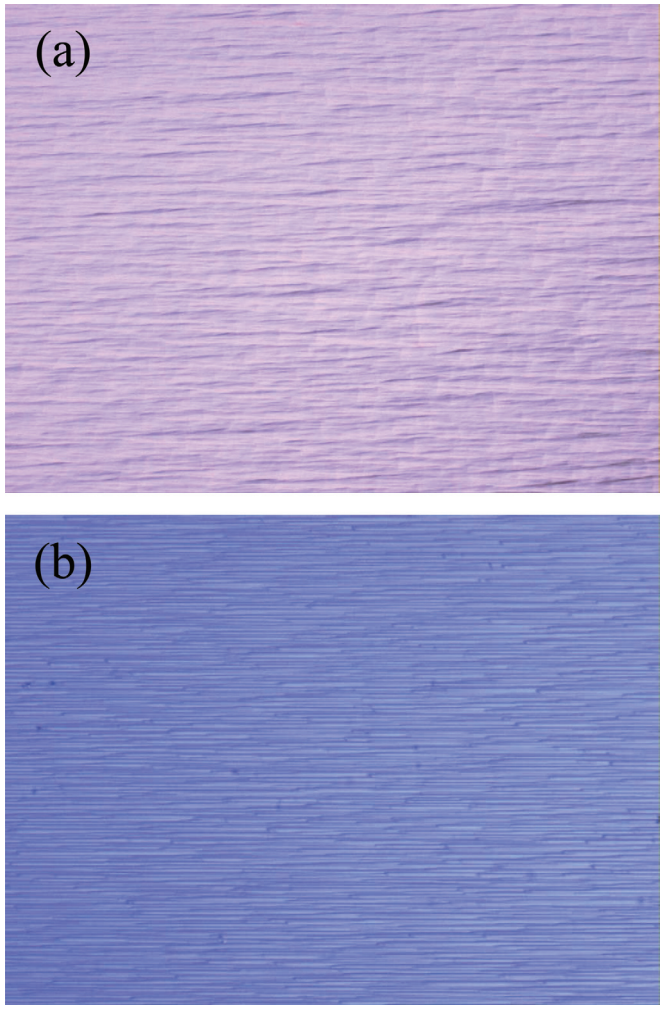

Figure 2. (Color online) Normarski optical contrast micrographs of (a) a-plane $(11\bar{2}0)$ and (b) semipolar $(11\bar{2}2)$ GaN films.

the dangling bond configuration of nitrogen on the surface is important to determine the selective etching of the polar GaN surface. Ga-face (0001) GaN is inert to the etchants because three occupied N-dangling bonds prevent OH^- ions from attacking the Ga back bonds.

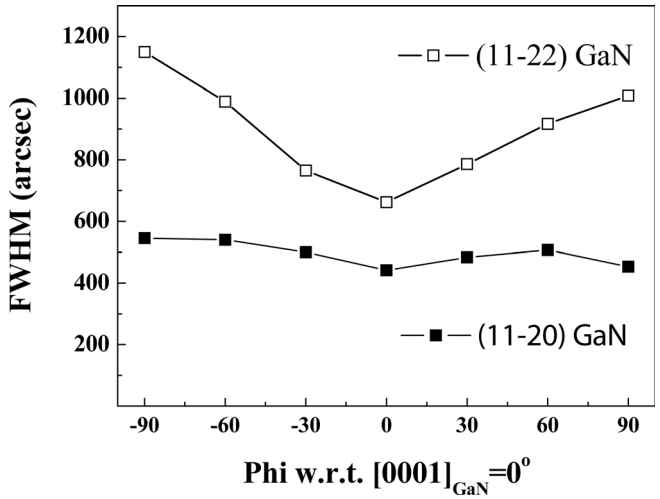

Figure 3. The full width at half-maximum plot of x-ray rocking curve of a-plane $(11\bar{2}0)$. GaN and semipolar $(11\bar{2}2)$ GaN films as a function of in-plane beam orientations.

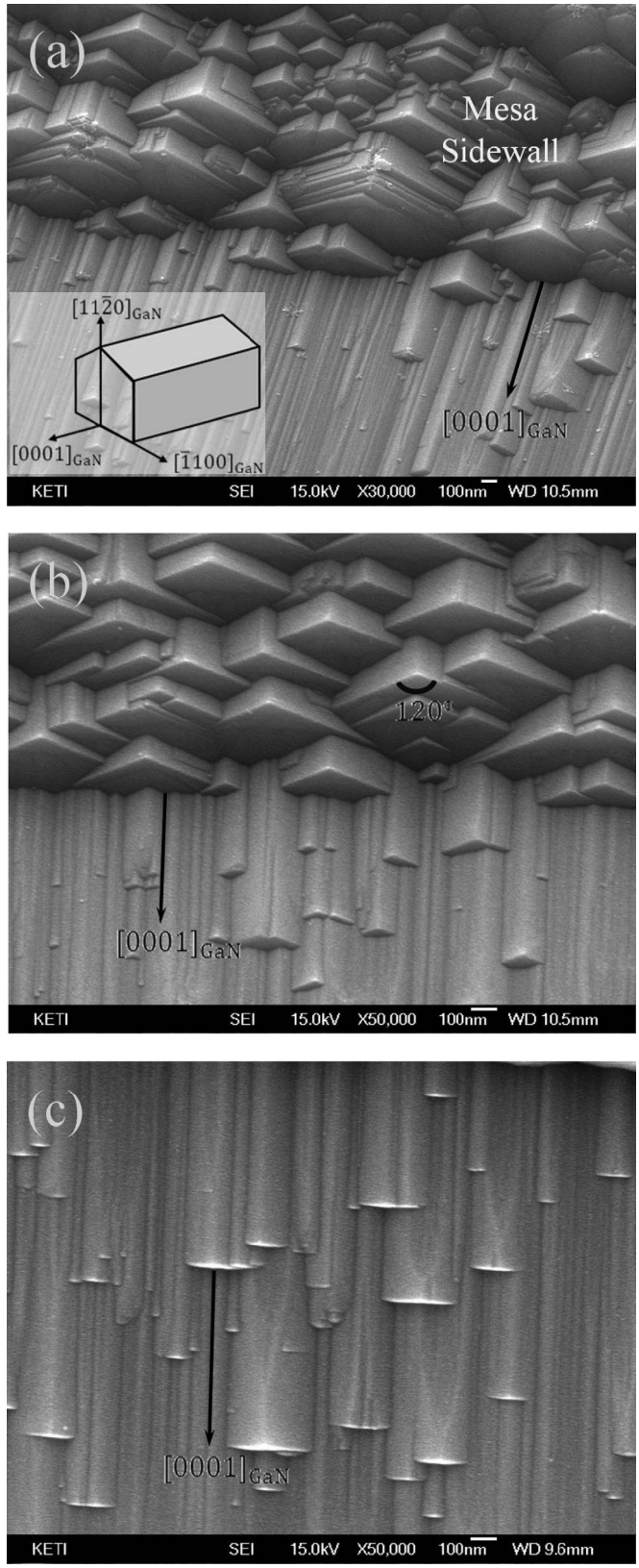

Figure 4. Tilted SEM images of etched a-plane $(11\bar{2}0)$ GaN films on (a) and (b) the mesa sidewalls along the c-axis direction and (c) the top surface.

It is quite interesting to see that specific crystallographic planes are exposed after PEC wet etching such as (0001), $(11\bar{2}2)$, $\{10\bar{1}0\}$, $\{10\bar{1}\bar{2}\}$, and $\{10\bar{1}\bar{1}\}$ planes.[24–28] These chemically stable planes are observed due to slower etch rates than other crystallographic planes

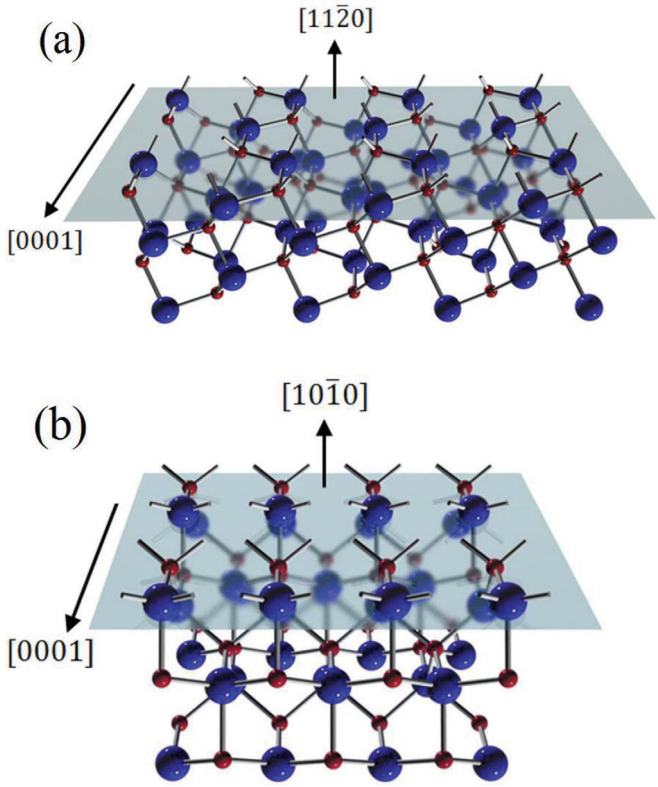

Figure 5. (Color online) Atomic bond configurations of (a) a-plane $(11\bar{2}0)$ GaN and (b) m-plane $(10\bar{1}0)$ GaN surfaces when viewed along the [0001] direction. Blue and red spheres represent Ga and N atoms, respectively.

during wet etching process. The $\{10\bar{1}\bar{1}\}$ planes of hexagonal pyramids are energetically stable due to smaller number of density of atoms than other planes.[16] PEC wet etching on the GaN films seems to proceed very slowly or even stop on chemically stable planes with a smaller density of atoms, especially when they are terminated with the Ga-dangling bonds.

Figure 2 shows Normarski optical contrast micrographs of the as-grown surfaces of the (a) a-GaN on r-plane sapphire and (b) s-GaN films on m-plane sapphire substrates. Both the films show a striated surface features in the direction perpendicular to the m-axis direction. The average root-mean-square (rms) surface roughness was measured to be 1–3 nm for the a-GaN films and 10–15 nm for the s-GaN films, as measured over a 2×2 μm^2 by atomic force microscopy. The full widths at half-maximum (fwhm) of x-ray rocking curve were obtained to study the crystalline quality of both the GaN films. As shown in Fig. 3, the observed fwhm values for the nonpolar a-GaN film were 441 arcsec in the c-axis direction and 452 arcsec in the m-axis direction. In the case of semipolar s-GaN film, the fwhm values were more anisotropic for the different azimuth angles and measured to be 662 arcsec and 1005 arcsec in the direction perpendicular and parallel to the m-axis direction, respectively.

Figures 4a and 4b show tilted SEM images of mesa sidewall morphologies of the nonpolar a-GaN films after 7 min of PEC etching. Trigonal prisms with various widths from 0.3 to 1.2 μm were heavily stacked on the mesa sidewall along the +c-axis [0001] direction, which correspond to the upper part of the unit cell of the a-GaN crystal structure. Note that 0.7-μm deep sidewall trench was intentionally formed with dry etching to see how each facet of tapered sidewall develops after PEC wet etching. Prismatic planes of $(10\bar{1}0)$ and $(01\bar{1}0)$ are clearly observed, indicating that the normal plane is the a-plane $(11\bar{2}0)$ and the m-plane family $\{10\bar{1}0\}$ is as chemically stable as + c-plane (0001). Typical hexagonal pyramids are seen on the mesa sidewall along the –c-axis $[000\bar{1}]$ direction. The stable m-planes are observed on the mesa sidewall along the +m-axis direction as well as and – m-axis direction (not shown here). Figure 4c shows the top surface morphology of the etched a-GaN films with long-striated trigonal prisms, which became smaller in widths by 100–300 nm. It is not clear why the dimensions of trigonal prisms on the top surface of the a-GaN film got smaller when compared with those on the tapered sidewall along the + c-axis direction. It is speculated that OH^- ions are not likely to break the Ga-back bonds, which are bound with N bonds in the a-GaN surface, as can be seen in Fig. 5a. Thus, the trenched sidewalls along the c-axis might be more favorable for wet etching to proceed because Ga-N chains are cut and dangling bonds are exposed on the sidewall facet.

Figures 5a and 5b show the three-dimensional ball and stick representation of the nonpolar a-GaN and m-GaN surfaces when viewed along the +c-axis [0001] direction, respectively. Blue and red spheres represent Ga and N atoms, respectively. An equal number of threefold coordinated Ga and N atoms are present on both nonpolar surfaces. While Ga–N dimers with two dangling bonds per each atom stand alone on m-GaN surface, Ga–N dimers with one dangling bond per each atom are bonded each other with zigzag chains on the a-GaN surface aligned along the c-axis direction. It is also notable that the density of atoms of the m-GaN surface (0.61×10^{15} cm^{-2} for each Ga and N atoms) is lower than that of the a-GaN surface (0.7×10^{15} cm^{-2} for each Ga and N atoms).

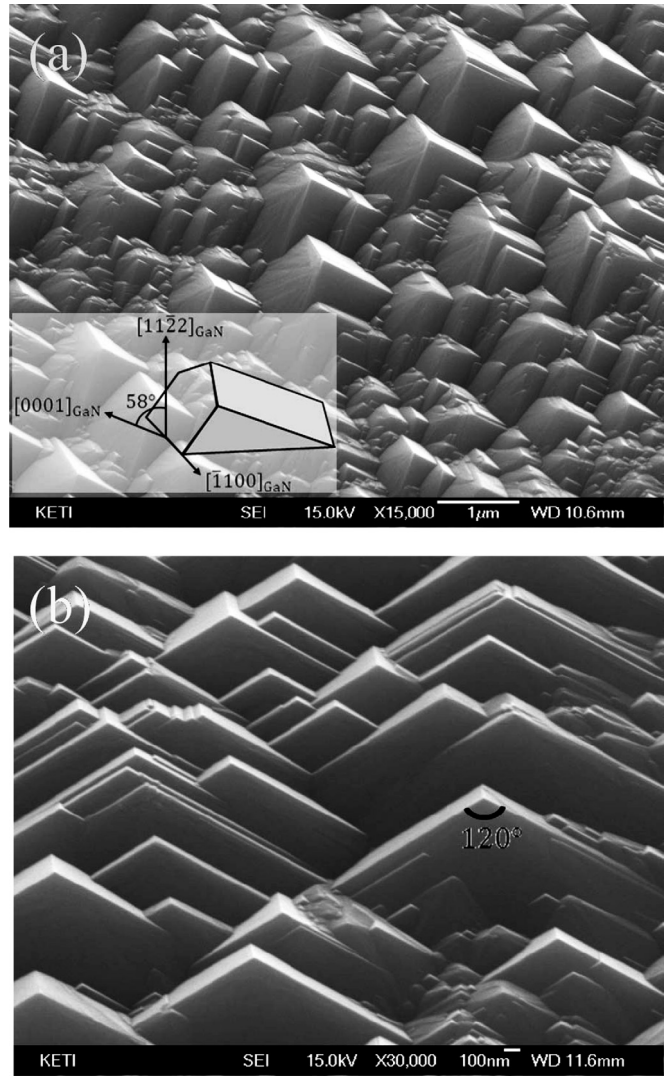

Figure 6. Tilted SEM images of etched surfaces of semipolar $(11\bar{2}2)$ GaN films from (a) the m-axis and (b) the c-axis directions.

The m-GaN is more energetically favored due to a lower surface energy (118 meV for m-GaN and 124 meV for a-GaN).[29] Thus, we speculate that the m-GaN surfaces are more chemically stable due to lower density of atoms and atomic bond configuration.

Figure 6a shows a titled SEM image of the etched surface morphology of s-GaN films after 5 min of PEC wet etching. As presented in the inset of Fig. 6a, it shows a lot of inclined trigonal unit cells embedded on the s-GaN surface. The chemically stable $(10\bar{1}0)$, $(01\bar{1}0)$, and (0001) planes are observed in common with the a-GaN films after PEC wet etching. It is notable that the etching is still under way on the c-plane (0001) surface whereas the m-GaN surfaces are clearly exposed. Figure 6b is a SEM image of the textured s-GaN surface in the + c-axis [0001] direction. Clear-cut m-GaN surfaces with a smooth morphology can be seen, ranging from 0.4 to 2.1 μm. The interplanar angle of 120° made between the m-GaN planes confirms that both planes are $(10\bar{1}0)$ and $(01\bar{1}0)$, which is the same case as Fig. 2. Defects-assisted PEC wet etching might proceed on the a-GaN and s-GaN films until chemically stable m-GaN surfaces as well as + c-plane (0001) GaN surface are exposed.

Conclusions

The etched surface morphologies of the heteroepitaxial nonpolar a-plane $(11\bar{2}0)$ and semipolar $(11\bar{2}2)$ GaN films are studied after photoenhanced chemical wet etching. Striated trigonal prisms with submicron widths are observed on the top surface and the sidewall facet along the c-axis direction for the nonpolar a-GaN film. Inclined trigonal unit cells are clearly exposed on the semipolar s-GaN films after PEC wet etching. The specific crystallographic planes of $(10\bar{1}0)$, $(01\bar{1}0)$, and (0001) were exposed in common for both GaN films, indicating that these planes are chemically stable due to smaller density of atoms and atomic bond configurations. Surface texturing with photoenhanced chemical wet etching can also be employed to enhance the performance of light emitting diodes and solar cells based on the nonpolar and semipolar GaN surfaces.

Acknowledgments

The authors thank Hye Jin Park at the FE-SEM analysis center in Korea Electronics Technology Institute. We also like to thank Professor Jun Seok Ha at the Chunnam University for helpful discussions and the guidance about nonpolar and semipolar GaN surfaces. The research at Korea University was supported by Basic Science Research Program through the National Research Foundation of Korea (NRF) funded by the Ministry of Education, Science and Technology (2010–0008242). This work was also supported by the Industrial Strategic Technology Development Program (10031811) by the Ministry of Knowledge and Economy (MKE, Korea).

Korea Electronics Technology Institute assisted in meeting the publication costs of this article.

References

1. F. Bernardini and V. Fiorentino, *Phys. Rev. B*, **56**, R10024 (1997).
2. P. Waltereit, O. Brandt, A. Trampert, H. T. Grahn, J. Meinnger, M. Ramsteiner, M. Reiche, and K. H. Ploog, *Nature*, **406**, 865 (2000).
3. T. Detchprohm, M. Zhu, Y. Li, Y. Xia, C. Wetzel, E. A. Preble, L. Liu, T. Paskova, and D. Hanser, *Appl. Phys. Lett.*, **92**, 241109 (2008).
4. S.-M. Hwang, Y. G. Seo, K. H. Baik, I.-S. Cho, J. H. Baek, S. Jung, T. G. Kim, and M. Cho, *Appl. Phys. Lett.*, **95**, 071101 (2009).
5. A. Chakraborty, B. A. Haskell, S. Keller, J. S. Speck, S. P. DenBarrs, S. Nakamura, and U. K. Mishra, *Jpn. J. Appl. Phys.*, **44**, L173 (2005).
6. M. Funato, M. Ueda, Y. Kawakami, Y. Narukawa, T. Kosugi, M. Takahashi, and T. Mukai, *Jpn. J. Appl. Phys.*, **45**, L659 (2006).
7. B. Neubert, T. Wunderer, P. Bruckner, F. Scholz, M. Feneberg, F. Lipski, M. Schirra, and K. Thonke, *J. Cryst. Growth*, **298**, 706 (2007).
8. M. Schmidt, K.-C. Kim, H. Sato, N. Fellows, H. Masui, S. Nakamura, S. P. DenBaars, and J. S. Speck, *Jpn. J. Appl. Phys.*, **46**, L126 (2007).
9. K.-C. Kim, M. C. Schmidt, H. Sato, F. Wu, N. Fellows, M. Saito, K. Fujito, J. S. Speck, S. Nakamura, and S. P. DenBaars, *Phys. Status Solidi (RRL)*, **1**, 125 (2007).
10. Y. Saito, K. Okuno, S. Boyama, N. Nakada, S. Nitta, Y. Ushida, and N. Shibata, *Appl. Phys. Express*, **2**, 041001 (2009).
11. Y.-D. Lin, A. Chakraborty, S. Brinkley, H. C. Kuo, T. Melo, K. Fujito, J. S. Speck, S. P. DenBaars, and S. Nakamura, *Appl. Phys. Lett.*, **94**, 261108 (2009).
12. H. Masui, S. Nakamura, S. P. DenBaars, and U. K. Mishra, *IEEE Trans. Electron Devices*, **57**, 88 (2009).
13. M. S. Minsky, M. White, and E. L. Hu, *Appl. Phys. Lett.*, **68**, 1531 (1996).
14. C. Youtsey, I. Adesida, and G. Bulman, *Appl. Phys. Lett.*, **71**, 2151 (1997).
15. H. M. Ng, N. G. Weimann, and A. Chowdhury, *J. Appl. Phys.*, **94**, 650 (2003).
16. D. Zhuang and J. H. Edgar, *Mater. Sci. Eng. R*, **48**, 1 (2005).
17. A. C. Tamboli, A. Hirai, S. Nakamura, S. P. DenBaars, and E. L. Hu, *Appl. Phys. Lett.*, **94**, 151113 (2009).
18. A. C. Tamboli, M. C. Schmidt, A. Hirai, S. P. DenBaars, and E. L. Hu, *J. Electrochem. Soc.*, **156**, H767 (2009).
19. M. T. Hardy, K. M. Kelchner, Y.-D. Lin, P. S. Hsu, K. Fujito, H. Ohta, J. S. Speck, S. Nakamura, and S. P. DenBaars, *Appl. Phys. Express*, **2**, 121004 (2009).
20. Y. Jung, M. Mastro, J. Hite, C. R. Eddy, Jr., and J. Kim, *Thin Solid Films*, **518**, 1747 (2009).
21. T. Fujii, Y. Gao, R. Sharma, E. L. Hu, S. P. DenBaars, and S. Nakamura. *Appl. Phys. Lett.*, **84**, 855 (2004).
22. Y. Gao, T. Fujii, R. Sharma, K. Fujito, S. P. DenBaars, S. Nakamura, and E. L. Hu, *Jpn. Appl. Phys.*, **43**, L637 (2004).
23. D. Li, M. Sumiya, S. Fuke, D. Yang, D. Que, Y. Suzuki, and Y. Fukuda, *J. Appl. Phys.*, **90**, 4219 (2001).
24. D. A. Stocker, E. F. Shubert, and J. M. Redwing, *Appl. Phys. Lett.*, **73**, 2654 (1998).
25. D. A. Stocker, I. D. Goepfert, E. F. Shubert, K. S. Boutros, and J. M. Redwing, *J. Electrochem., Soc.*, **147**, 763 (2000).
26. Y. Gao, M. D. Craven, J. S. Speck, S. P. DenBaars, and E. L. Hu, *Appl. Phys. Lett.*, **84**, 3322 (2004).
27. M. Itoh, T. Kinoshita, C. Koike, M. Takeuchi, K. Kawasaki, and Y. Aoyaki, *Jpn. J. A ppl. Phys.*, **45**, 3988 (2006).
28. S. Kitamura, K. Hiramatsu, and N. Sawaki, *Jpn. J. Appl. Phys.*, **34**, L1184 (1995).
29. J. E. Northrup and J. Neugebauer, *Phy. Rev. B*, **50**, R10477 (1996).